

Encoding electronic structure information in potentials for multi-scale simulations: SiO₂

Wuming Zhu^a, D.E. Taylor^a, A.R. Al-Derzi^a, K. Runge^a, S.B. Trickey^{a,*},
Ju Li^b, Ting Zhu^c, S. Yip^d

^a Quantum Theory Project, Departments of Physics and of Chemistry, P.O. Box 118435, University of Florida, Gainesville, FL 32611-8435, United States

^b Department of Materials Science and Engineering, Ohio State University, Columbus, OH 43210, United States

^c Woodruff School of Mechanical Engineering, Georgia Institute of Technology, Atlanta, GA 30332, United States

^d Department of Nuclear Science and Engineering, Massachusetts Institute of Technology, Cambridge, MA 02139, United States

Received 24 February 2005; accepted 3 October 2005

Abstract

Potentials generally used in molecular dynamics (MD) simulation of SiO₂ properties customarily are calibrated to a combination of computed molecular electronic structure data and experimental crystalline data. The present study tests parametrization to data from high-level, first-principles electronic structure calculations *alone*. The issue is crucial to the success of multi-scale simulations. They require a consistent embedding of the so-called quantum mechanical region (the region in which the forces come from gradients of quantum mechanical total energies) in a classical inter-ionic potential region. The evident challenge is generation of a *quantum mechanically consistent* parametrization. A simple probe of the issue is to see how parametrization solely from first-principles data influences the simulation outcomes. We parametrized a widely used form of effective inter-ionic potential for SiO₂ and did MD simulations of tensile failure in a 72 formula unit SiO₂ nanorod. Separate parametrizations were done to high quality calculated data for H₄SiO₄ and H₆Si₂O₇ clusters and for α -quartz. The differing parametrizations yield quantitative differences in the prediction of the yield strength and even semi-qualitative differences in the system behavior in that region. Some superficially similar parametrizations do not even provide a stable $T = 0$ K configuration. These differences highlight the crucial distinction between potential parametrization aimed at *replacing* realistic quantum mechanical forces entirely in an MD calculation versus a parametrization aimed at *embedding* an explicitly QM region.

© 2006 Elsevier B.V. All rights reserved.

Keywords: Inter-atomic potentials; Multi-scale simulations; Silica simulations

1. Purpose

The broad success of molecular dynamics (MD) simulation of condensed phase properties rests upon inter-ionic potentials as effective substitutes for the explicit quantum mechanics (QM) of bonding by electrons [1,2]. SiO₂ is a technologically and scientifically important example [3]. There are many parametrized interactions for SiO₂ [4,5]. But the issues of interest in multi-scale simulations, our focus, are easily illustrated with the so-called TTAM [6]

and BKS [7,8] pair potentials. (The acronyms refer to the respective sets of authors.) These potentials are heavily cited in the materials literature, a fact that suggests they are viewed as successful by the materials simulation community [9]. The relationship of such potentials to QM is the general topic of this work.

As published, the TTAM and BKS potentials were parametrized to a combination of first-principles QM electronic structure results for a small cluster and experimental data for α -quartz [6–8]. The “TTAM/BKS” form is

$$U_{ij} = \frac{\kappa Q_i Q_j}{r_{ij}} + \alpha_{ij} \exp[-\beta_{ij} r_{ij}] - \frac{\gamma_{ij}}{r_{ij}^6} \quad (1)$$

* Corresponding author. Tel.: +1 352 392 1597; fax: +1 352 392 8722.
E-mail address: trickey@qtp.ufl.edu (S.B. Trickey).

where the ions i, j have relative displacement r_{ij} . Energies are in eV, lengths in Å, the Q_i are in units of electron charge magnitude, and κ is the conversion from electrons² per Å to eV (≈ 14.402). From their functional forms, the three terms are called Coulomb, Buckingham, and van der Waals terms, respectively. (Our notation differs from the originals to facilitate comparative presentation.)

While three-body interactions are known to be important for ceramics [5,10,11], the ultimate realism of the potential is not the issue for this study. Rather, we have a single, fundamental concern. Given a successful, popular form of potential, what are the effects of using different first-principles QM inputs for its parametrization? The context is multi-scale simulations. In them, the forces in a relatively small region, the so-called QM region, are generated by some choice of approximate QM method. The QM region is embedded in a much larger collection of particles for which the dynamics are determined by inter-ionic potentials, the “CM region”. Brenner [12] has given a comprehensive discussion of the issues of potential parametrization for ordinary MD simulations. Obviously those simulations do not involve embedding a QM region, the procedure of concern to us. The question is how to take QM into account in the parameterization of a classical potential.

Both BKS and TTAM used the same broad approach to parametrization but with significant differences in detail. Each group picked a terminated SiO_4 cluster but with different terminations. They then chose a specific QM approximation, Hartree–Fock (HF), to provide calibration data in the form of energy as a function of geometrical structure for their respective clusters. Each group then found multiple parameter sets that fit the chosen potential form to their respective QM data sets. From among those parameter sets, each group chose the set that yielded the best fit of certain calculated crystalline properties to experimental data. Details differ, but that is the essential scheme.

For a multi-scale calculation to be unequivocally predictive, there must be no reliance on experimental data. Achieving freedom from experimental calibration is closely related to the primary focus of this paper. Viewed in this way, the objective is to obtain the parameter set for a given potential that provides the best possible reproduction of calculated QM properties for a given choice of QM approximation. This is equivalent to pursuing the implicit logic of the BKS/TTAM approach to its end, that is, doing all the parameterization via QM.

The computed data reported in Ref. [13] show that an all-QM calibration is not an easy task. That study treated “chemically or physically appealing” $\text{H}_m\text{Si}_n\text{O}_q$ clusters. It found a wide variation in calibration data sets even if one restricts consideration to such clusters. The variation has two main sources. First, there is no unique choice of plausible reference cluster. Second, results for any particular cluster vary substantially depending upon choices of methodology (level of refinement of approximation, basis set size, etc.). The other possible extreme for a calibration

system, the perfect crystal alone, was studied in Ref. [14]. Comparison of the crystalline and cluster results in those two papers makes clear that calibration of the *same* potential form will yield significantly *different* parameters.

As an example of reference data differences, the best-quality molecular calculations of Ref. [13] give a range of 1.557–1.748 Å for the equilibrium Si–O bond length in 12 $\text{H}_m\text{Si}_n\text{O}_q$ clusters. This range is in sharp contrast with the α -quartz companion study [14], which obtained values of 1.628–1.638 Å. Clearly the question is, do these differences affect the MD results for a many-particle system significantly? We show here that the answer is unambiguously affirmative and characterize the differences.

Ultimately more than just an understanding of parametrization methods and logic is needed. A truly successful multi-scale simulation must have a way to calibrate (and adjust) the classical embedding potential consistent with the chemical reactions occurring in the QM region. This study of a priori, non-adaptive parametrizations therefore differs in its objective from the usual parametrization effort. The usual requirement is that the parametrization give MD results in accord with experiment. The parameter sets tested here are *not* intended nor expected to be superior to those already published for standard MD simulations. Rather it is the dependence of MD results on QM calibration procedures that we scrutinize.

2. Parametrizations

2.1. Cluster energetics

First we consider the consequences of parametrizing to cluster energies alone. This approach is appealing in part because of its strong connection with chemical transferability concepts. Use of cluster forces (instead of energies) is considered below.

It is helpful to distinguish what we call BKS-type and TTAM-type parametrizations. These differ by the absence of non-coulombic Si–Si interactions in BKS-type fits (BKS; $\alpha_{\text{Si-Si}} = \gamma_{\text{Si-Si}} = 0$) versus their presence in TTAM. Notice, however, that our use of “TTAM-type” does *not* signify an atom-by-atom additive parametrization, the procedure used by TTAM.

Because there is no unique a priori choice of parametrizing cluster, we used two intuitively relevant choices. For BKS-type fits, we chose the cluster BKS [7,8] used, H_4SiO_4 . Fitting purely to it is a test of the robustness of the BKS procedure without recourse to experimental crystalline data as a corrective. For TTAM-type fits, we chose $\text{H}_6\text{Si}_2\text{O}_7$. It tests the significance of including a real Si–Si interaction in a silica-like cluster. In contrast, were we to apply the logic of the TTAM atom-by-atom parametrization approach to their cluster, $\text{SiO}_4^{4-} + 4\text{e}^+$, alone, the odd result would be a non-Coulombic Si–Si interaction from a cluster with only one Si. (Also there is a technical reason for not using the cluster employed by TTAM: the bare terminating charges cause problems. See Ref. [13] for details.)

For reference, all the calculations on the BKS cluster, H_4SiO_4 , were done at the highest level of refinement (CCSD(T) with the richest basis set, aug-cc-pVDZ; see Ref. [13] for nomenclature and details). Our fitting followed the BKS prescription for handling the terminating H atoms. Namely, they were treated as scaled silicons in the pair potential, $Q_{\text{H}} = Q_{\text{Si}}/4$, with no other interaction. We calculated energies on a grid of 15 geometries around the computed equilibrium configuration: a single Si–O bond stretched by ± 0.4 , ± 0.2 Å, all four Si–O bonds uniformly dilated by ± 0.4 , ± 0.2 Å, and one O–Si–O bond angle distorted by $\pm 6^\circ$, $\pm 4^\circ$, and $\pm 2^\circ$.

The BKS cluster introduces an unanticipated, spurious termination effect. As shown in Ref. [13], a high-level calculation of the equilibrium H_4SiO_4 geometry has two *distinct* O–Si–O angles, 100.3° and 114.2° . This behavior, which did not occur in the original BKS calculation, is a consequence of H-termination and the resulting O–H interaction. The two distinct angles force the fitted O–O potential to compromise between a shorter and longer equilibrium O–O distance. The only way to do that with a pairwise potential (which has only a single extremum), Eq. (1), is via parameters that give an unphysical potential. Such behavior showed up severely in the actual parametrization: the fitted O–O potential has a local *maximum* at the minimum, 100.3° , of the CCSD(T) energy as a function of the smaller O–Si–O angle.

The BKS cluster energies as a function of geometric configuration and relative to the equilibrium energy are listed in Table 1. These were fit to the BKS/TTAM form Eq. (1) by least squares as implemented in the ROBMIN modules in the code ROBFIT [15,16]. Those modules minimize the fitting error with the Levenberg–Marquardt scheme [17], in essence, an algorithm for mixing inverse Hessian and steepest descent minimizations. The particular implementation in ROBMIN is unusual in three respects that proved important in the present work. First, each variable to be determined (here, each of the potential parameters) is assigned its own Marquardt weighting parameter. Second, optimum ratios of the Marquardt parameters for the next minimization step are determined by analysis of failed minimization steps. The overall Marquardt parameter is determined by the requirement that the predicted χ^2 be equal to the current χ^2 multiplied by a ratio that depends on the current rate of convergence of the fitting.

Table 1
Energy shifts (Hartree au) for the unconstrained BKS cluster, H_4SiO_4 from CCSD(T), aug-cc-pVDZ calculations as a function of geometry shift from calculated equilibrium

One $R_{\text{Si-O}}$	+0.2 Å	+ 0.4 Å	−0.2 Å	−0.4 Å		
ΔE	0.0163496	0.0487257	0.0324494	0.1953456		
All $R_{\text{Si-O}}$	+0.2 Å	+ 0.4 Å	−0.2 Å	−0.4 Å		
ΔE	0.0702095	0.2053619	0.1402291	0.8431855		
$\angle\text{O-Si-O}$	+2°	+ 4°	+ 6°	−2°	−4°	−6°
ΔE	0.0001836	0.00071141	0.0015581	0.0001944	0.0008015	0.0018650

See text.

Nonetheless, the fitting is difficult in two specific senses. It is hard to avoid spurious negative parameters. In particular, it is easy to obtain $\gamma_{\text{O-O}} < 0$. In the original BKS parametrization $\gamma_{\text{O-O}}$ was set to zero in the cluster part of the fit, then determined entirely from the crystalline part of their fitting procedure. Working with cluster data alone precludes this remedy.

The other major fitting problem is to decide how to weight configurations that energetically are far from equilibrium. Note Table 1 again. This weighting issue does not seem to have been addressed in earlier work. Eventually we settled on an inverse linear weighting $w_i = (E_1 - E_0)/(E_i - E_0)$ where E_0 is the calculated equilibrium total energy and E_i are the energies of the strained configurations, with $i = 1$ the strained configuration nearest in energy to E_0 . The resulting parameters are in Table 2. We do *not* recommend these parameters for materials simulations because of the unphysical O–O local maximum just discussed as well as the general grounds mentioned earlier.

One way to evade the problem of two O–O equilibrium separations is to use the “tetrahedrally constrained” (“tc”) cluster results from Ref. [13]. Those calculations used the same method and basis on a BKS H_4SiO_4 cluster held at the tetrahedral O–Si–O geometry and with the terminating Hs cyclic at the dihedral angle found by BKS. The imposed symmetry of course resolves the O–O problem but at a considerable cost in strain energy; see Ref. [13]. The symmetry constraint also decouples the bond stretch (T_d) and angular (D_{2d}) modes of motion for fitting. Calculated energies on a grid of 14 bond lengths and 17 angles went into the fit. The resulting parameters are in Table 3.

In addition to the general caution about recommending any of these parameter sets, there is a strong reason to distrust this particular set. The minimum of the fitted energy

Table 2
Parameters of the BKS type for silica from fitting to energetics of the unconstrained H_4SiO_4

	Q	α_{ij}	β_{ij}	γ_{ij}
Si–Si	2.0267	0	0	0
Si–O		18003.799	4.74236	133.7342
O–O	$-Q_{\text{Si}}/2$	1388.7787	3.92408	242.4551

See text for cautionary notes. Q_i in units of electron charge, α_{ij} in eV, β_{ij} in Å^{-1} , γ_{ij} in eV Å^6 .

Table 3
Parameters of the BKS type for silica from fitting to energetics for the “tetrahedrally constrained” H_4SiO_4 cluster

	Q	α_{ij}	β_{ij}	γ_{ij}
Si–Si	2.4	0	0	0
Si–O		7293.45	4.7938	25.980
O–O	$-Q_{\text{Si}}/2$	1301.98	2.6898	329.428

See text for details. Units as in Table 2.

occurs at a notably larger angle, about 117° , than the minimum in the reference data. Curiously, the published BKS parameters have the same flaw. Fig. 1 displays the problem. Notice in particular that the fitted parameters give a potential that replicates the bond stretch energetics much better than the published parameters but that both sets miss the minimum in the angular energetics. (Notice that the zeros of energy have been shifted to match in Fig. 1. The published BKS and TTAM parameters give a zero of energy that differs drastically from the separated atom limit of the molecular or crystalline calculations.)

Turning to the TTAM-type fitting, we chose $\text{H}_6\text{Si}_2\text{O}_7$ as the reference molecule in part because it had been used as a surrogate for silica energetics since at least the work of Newton and Gibbs [18]. A pertinent review from that period is by Gibbs [19]. More recently Wong-Ng et al. [20] modeled some aspects of silica fracture mechanics based on Restricted Hartree–Fock (RHF) calculations for $\text{H}_6\text{Si}_2\text{O}_7$. Moreover, this molecule does provide information on the Si–Si interaction. In the present work, the calculated molecular energies (in the CCSD approximation) were for

12 conformations: equilibrium plus 11 stretches of a single Si–O bond [13]. This relatively small sample of configurations illustrates the limits imposed by computational cost. In particular, detailed exploration of the weak dependence on the central Si–O–Si angle would have been very costly. See Ref. [13] for details. However, the relative success of a quantum mechanical Hamiltonian parametrized to the stretching data alone [21] was encouraging.

TTAM-type fitting for clusters is complicated by the fact that β_{ij} values in the vicinity of the TTAM value tend to make the total potential energy rather insensitive to the prefactor α_{ij} . If Q_{Si} also is kept as a variational parameter, this fitting instability generally worsens. Since the primary issue for this part of the study was the Si–Si interaction, we would have preferred to address the issue by fixing all of the other parameters (Si–O, O–O) to the published TTAM values. Then with a starting value for Q_{Si} , the parameters $\alpha_{\text{Si–Si}}$, $\beta_{\text{Si–Si}}$, and $\gamma_{\text{Si–Si}}$ could be fitted. This approach fails because the Si–Si distances are always such that the Si–Si potential is sampled only in its tail. The potential is quite flat there and the fitting is ill-posed. Two other fits do work, at least in the sense of providing a reasonably close representation of the CCSD energy as a function of bond distance. One is to fit only the Si–O parameters, the other is to fit both Si–O and Si–Si parameters. For the latter case we tried both $Q_{\text{Si}} = 2.4$ and 2.6 with relatively little effect on the overall quality of fit. In both cases all other parameters were fixed at published TTAM values. Notice that implicitly this forces a reliance on experimental data. The parameters that result are in Table 4.

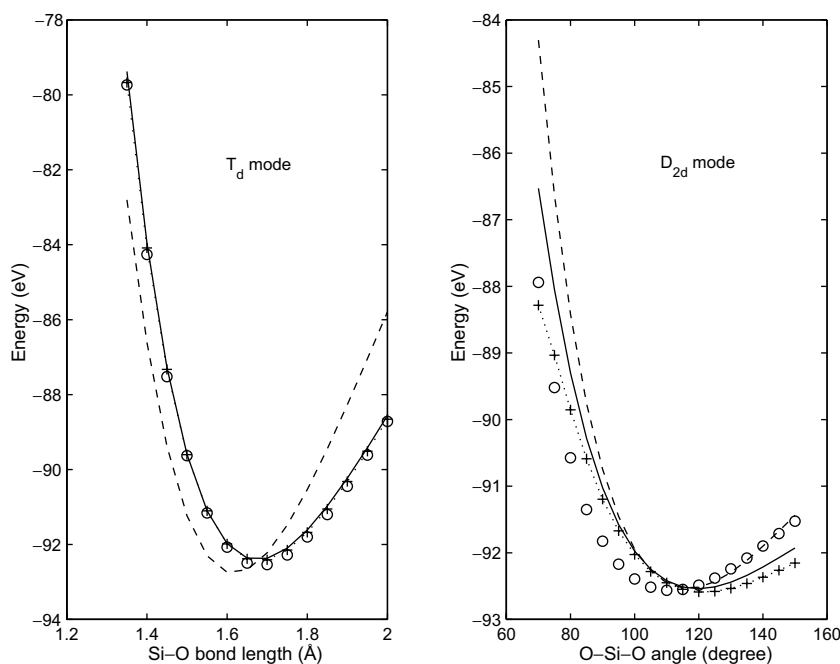


Fig. 1. Energies (eV) for tetrahedrally constrained H_4SiO_4 as a function of bond length (Å; T_d mode) and bond angle (degrees; D_{2d} mode). Open circles are data from high-level calculations, “CCSD(T)”. Crosses connected by the dotted curve corresponds to BKS-type parameters obtained by fit to the CCSD(T) energies. Dashed curve is from published BKS parameters. Continuous curve is from fits to CCSD(T) energy gradients. To have a common zero, CCSD(T) energies are shifted by 16,012 eV and fitted energies by -6.8 eV; see text and Tables 3 and 4.

Table 4
Parameters of the TTAM type for Silica from fits to $H_6Si_2O_7$

	Q	α_{ij}	β_{ij}	γ_{ij}
Si–Si	2.4 (chosen)	8.729×10^8	15.2187	4502.541
Si–O		10677.686	4.39775	110.039
O–O	$-Q_{Si}/2$	1758.02	2.84641	214.877
Si–Si	2.6 (chosen)	8.729×10^8	15.3768	3869.636
Si–O		10062.449	4.35293	107.317
O–O	$-Q_{Si}/2$	1758.02	2.84641	214.877

See text regarding Q_{Si} and the O–O parameters. Units as in Table 2.

2.2. Crystal energetics

The procedure for fitting to the computed α -quartz data from Ref. [14] was essentially the same as the energetic fit for the clusters, with the additional aspect of lattice summation. Ewald summation did not prove necessary; a simple summation by shells of neighbors until the next additional contributions were below machine precision sufficed. The resulting fits are shown in Table 5 for both Perdew–Burke–Ernzerhof (PBE) gradient dependent approximation and Hedin–Lundqvist (HL) approximations to the exchange-correlation energy E_{xc} of density functional theory. Details of these and other calculational matters are in Ref. [14].

In addition to the fitting issues summarized already, the γ_{ij} are difficult to fit to approximate DFT energies. Exact DFT would yield a van der Waals tail for asymptotically large lattice parameters. Approximate exchange-correlation energy kernels, such as those used in Ref. [14], cannot reproduce that exact asymptotic behavior. Those approximations are local functionals of the charge density and its gradients. Far from any nucleus, the density decays as $\exp[-Cr]$, so the overlap density in that region also decays exponentially, hence the asymptotic decay of the approximate E_{xc} and the DFT E_{tot} is exponential also. The practi-

Table 5
Parameters as fit to the PBE and HL energetics for α -quartz

	q	α_{ij}	β_{ij}	γ_{ij}
PBE, BKS-type				
Si–Si	2.5533	0	0	0
Si–O		10801.333	4.76156	59.9106
O–O	$-Q_{Si}/2$	1559.1159	3.12569	95.8142
HL, BKS-type				
Si–Si	2.3854	0	0	0
Si–O		10798.007	4.83689	56.9642
O–O	$-Q_{Si}/2$	1689.0676	3.27648	78.6577
PBE, TTAM-type				
Si–Si	2.4266	8.61588×10^8	15.2183	23.2603
Si–O		10658.861	4.7199	70.6100
O–O	$-Q_{Si}/2$	828.9556	2.6117	214.370
HL, TTAM-type				
Si–Si	2.4172	8.61588×10^8	15.1592	23.2603
Si–O		10683.035	4.74821	70.6100
O–O	$-Q_{Si}/2$	1131.0659	2.73986	214.370

“BKS-type” and “TTAM-type”: see text. Units as in Table 2.

cal problem is worst for γ_{Si-Si} simply because the mean Si–Si separation is larger than for O–O or Si–O.

Though unmentioned by TTAM [6], their procedure in fact had a similar problem for Si–Si because they used HF energies. Those cannot have a van der Waals tail either. TTAM’s additive parametrization masked the problem. (BKS [7,8] did not have the problem because they assumed $\alpha_{Si-Si} = \gamma_{Si-Si} = 0$.) For TTAM-type fits to the α -quartz computed data, we were unable to find a sensible, non-zero set of Si–Si parameters with γ_{Si-Si} as one of the fitting variables. Attempts to do so always led to nonsensical, negative values of the parameters α_{Si-Si} , β_{Si-Si} . As a pragmatic route to a TTAM-type fit therefore, we set γ_{Si-Si} to roughly the TTAM value and fitted the remaining parameters to the α -quartz DFT results. For BKS-type fits, which have several parameters fixed by design, we were able to find reasonable values of the γ_{ij} when calibrated to the α -quartz computed data.

None of the parameter sets, either BKS- or TTAM-type, that result from fitting to crystalline calculations much resembles the published values however. Note particularly the gross variation in the α_{O-O} parameters for TTAM-type fits to energetics from the PBE versus HL approximate density functionals. In contrast, the BKS-type Q_{Si} from PBE is reasonably close to the natural atomic orbital population found in Ref. [13], while the BKS-type fit to HL data and both TTAM-type fits are close to the value of 2.4 used by both TTAM and BKS. Consequences of these differences are pursued in Section 3.

2.3. Cluster forces

Since proper embedding of a QM region in an MD simulation is the objective, fitting to computed forces (energy gradients) might be superior to fitting to computed energies. The two approaches obviously are equivalent on an arbitrarily dense grid. But on a finite grid, the forces at a point correspond to the infinitely dense mesh limit of energy differences at multiple grid points. Therefore if computed forces are available from the electronic structure calculation it is uneconomical to ignore them. Also there is a seemingly trivial but operationally important advantage to calibration against computed forces. In fitting to computed energies, the zero of energy in the electronic structure calculation (cluster or solid) differs from the zero for the sum over pair potentials by a constant. Since that constant offset is unknown a priori, it must be obtained by the fitting procedure even though it is irrelevant so far as embedding the dynamics is concerned. Obviously that does not happen with calibration to forces.

Most modern molecular codes provide “analytical gradients”. This is quantum chemistry jargon which signifies that, for each nuclear configuration, the code computes force components from analytical expressions for the gradient of whatever approximation to the QM total energy was chosen. Typically the gradient components are with respect to internal molecular coordinates, a tedious

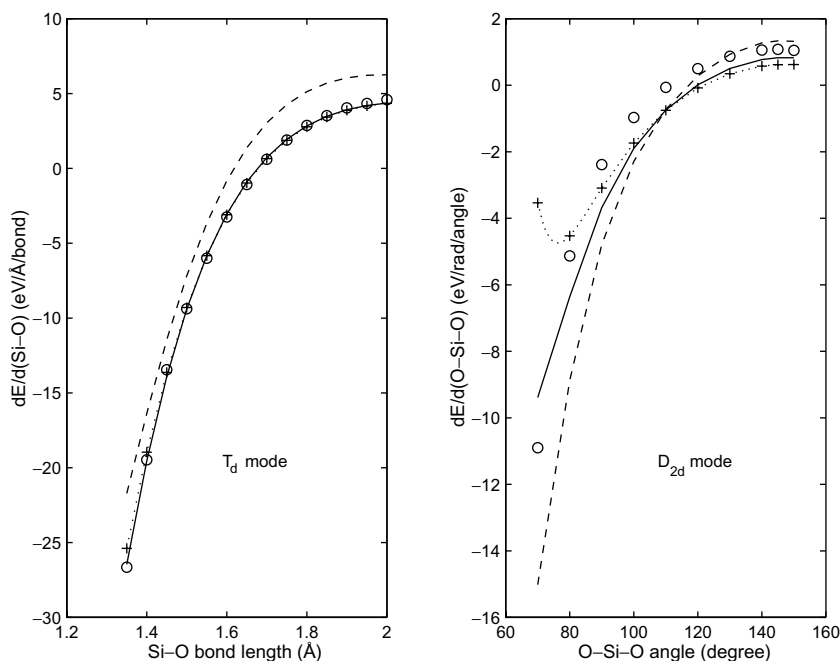


Fig. 2. Computed gradients with respect to bond stretch and angular motions of H_4SiO_4 . Symbols as in Fig. 1.

nuisance but not a true barrier. Such is the case with the ACES-II code [22] we used. Analytical gradients are relatively uncommon in periodic codes. Fitting function algorithms, such as in the code GTOFF we used [23], have a particularly difficult technical problem of dealing with so-called Pulay forces associated with the fitting functions. Thus GTOFF does not have analytical gradients, so this part of the study was restricted to the molecular clusters.

Once again, we primarily used the “tc” H_4SiO_4 BKS cluster. Gradients for distortions of H_4SiO_4 with the published BKS parameters, turn out to be closer to the CCSD(T) gradients than might have been supposed (see Fig. 2). Notice that the fitted parameters reproduce the T_d force components from the electronic structure calculations almost exactly, whereas the published parameters are too stiff. However the fitted parameters do only a little better than published ones for the D_{2d} force component. The comparison is a bit surprising because the original BKS fit used cluster reference energies computed at a lower level of theoretical refinement, RHF, than was used here, CCSD(T). Details are in Ref. [13].

With the published parameters as a starting point, we are able to generate a set of fitted parameters that repro-

duces the T_d gradients almost exactly but still has a problem with D_{2d} gradients. The resulting parameters are displayed in Table 6. As was shown in Fig. 1, the energetics that those parameters yield reproduce the CCSD(T) T_d motion energetics quite well (without any zero shifting), but mislocate the minimum in the D_{2d} motion.

3. MD simulations

3.1. System and methods

For a simple comparative test of the effect of different parametrizations on calculated materials properties, we considered the tensile fracture of silica nanorods. The system building block is a modular ring of $\text{Si}_6\text{O}_{12} = 6 * \text{SiO}_2$, with 6 Os in the Si ring plane, and, formally, 3 above and 3 below (alternatively, six above and six below, both shared with the next module up or down). Each end cap is built similarly, from a full SiO ring filled out with 3 alternating bridging Os, corresponding to $12 + 3 + 6/2 = 18$ atoms per end cap. The topmost (or bottommost) 15 atoms in each endcap are fixed for longitudinal motion; see below. Hence we refer to “15-atom” endcaps. Two versions of this system were used: a 36 formula unit (108 atom) nanorod consisting of four Si_6O_{12} modular rings subject to extension plus the two caps and a 72 formula unit (216 atom) system with ten Si_6O_{12} rings subject to extension and the same capping. Only results for the larger system are presented here (there was no substantive difference in the behavior of the smaller one).

The particular nanorod configuration (stacks of 6-member rings) is designed to mimic quartz. It consists of tetrahedra such that each Si has four neighbors and each O two.

Table 6
Parameters of the BKS type for silica from fitting to forces for the “tetrahedrally constrained” H_4SiO_4 cluster

	Q	α_{ij}	β_{ij}	γ_{ij}
Si–Si	2.40	0	0	0
Si–O		7149.17	4.7864	27.661
O–O	$-Q_{\text{Si}}/2$	1359.30	2.8086	215.829

See text for details. Units as in Table 2.

Hence there are no dangling bonds nor artificial terminations and the system is chemically plausible. Additional motivation for treating these nanorods arises from the fact that they are the minimal molecular-scale system with meaningful mechanical properties (e.g. Young's modulus) usually associated with an extended system. Intermediate in size between molecules and the bulk, these nanorods are tractable with all three simulation techniques: empirical potentials, quantum chemical electronic structure calculations, and DFT periodically-bounded supercell calculations [24].

Each simulation began by Broyden–Fletcher–Goldfarb–Shanno [25] energy minimization at $T = 0$ K. If a stable structure were found, then it became the initial configuration for the MD. MD was not attempted on any system without a stable $T = 0$ K structure. During the MD runs, the axial coordinates (z) of the endcap atoms were fixed at their $T = 0$ K values. All other coordinates (x, y for endcap atoms, x, y , and z for others) then were relaxed for 1000 time steps. The temperature was held at $T = 5$ K by velocity rescaling whenever the kinetic temperature deviated by more than 1 K. Time steps of 2.15 fs were used; testing showed no significant change with use of much shorter steps. At each time step after equilibration, the nanorods were elongated by an increment equivalent to a strain rate of 5 m/s until and well beyond failure. The MD code [26] uses the sixth-order Gear predictor–corrector integrator [1,27].

3.2. Calculated stress–strain curves

The published BKS and TTAM parameters give a stable equilibrium nanorod of the type shown in Fig. 3. Unsurprisingly, the BKS-type fit to the energetics for the unconstrained H_4SiO_4 does not give a stable $T = 0$ K equilibrium configuration. This follows from the unphysical character of the O–O interaction generated by the parameters in Table 2. Recall discussion above. More significantly, the BKS-type parameters fitted by energy criteria to “tc” H_4SiO_4 also fail to yield a stable $T = 0$ K equilibrium nanorod. In this case the problem is a bit more subtle. Study of Figs. 1 and 2 helps in understanding. The fitted potential is too repulsive for angular compressions and too weak for large angular expansions. As a result the system will not stay together. Presumably the published parameters are better in this regard because of the corrective influence of experimental crystalline data.

Neither of the TTAM-type fits tabulated in Table 4 will give a stable 216-nanorod either. Here the difficulty seems to be related to the Si–Si interaction problem discussed above. It may also be that the restriction of calibration data to a single bond stretch is a factor. Considering other distortions would have been computationally prohibitive however.

Fig. 4 gives a comparison of the stress–strain behavior of all the BKS-type fits that work, namely gradient fit to

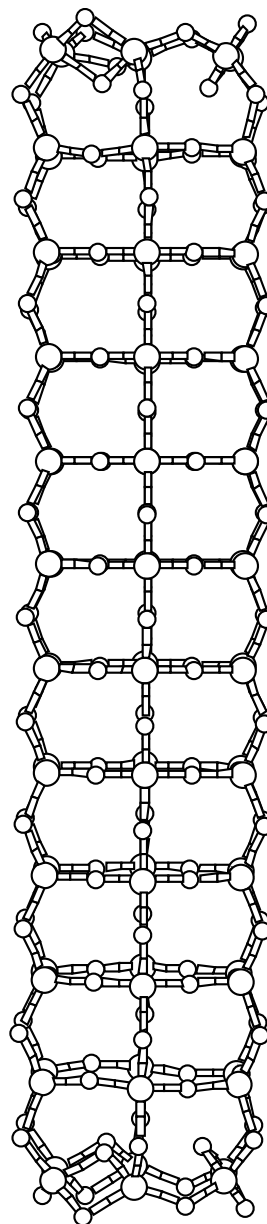


Fig. 3. The equilibrium 216-atom silica nanorod.

“tc” H_4SiO_4 and α -quartz fits. Fig. 5 gives TTAM-type results. There are clear qualitative differences. Published BKS parameters give the highest yield strength by far, perhaps not surprising in view of Fig. 1, especially for T_d .

The HL and PBE fits differ relatively little but are substantially different from the published BKS parameter set. Most notable is the gradient-fitted BKS set, which gives roughly two-thirds the yield strength of the nanorod (at slightly lower failure strain) versus the published-BKS-parameters. Comparison of Figs. 4 and 5 show a curious behavior for the gradient fitted BKS-type potential. It gives essentially the same failure strain as published TTAM parameters but at about 10% lower yield strength. This is a stark example of the non-uniqueness of single-cluster parametrization.

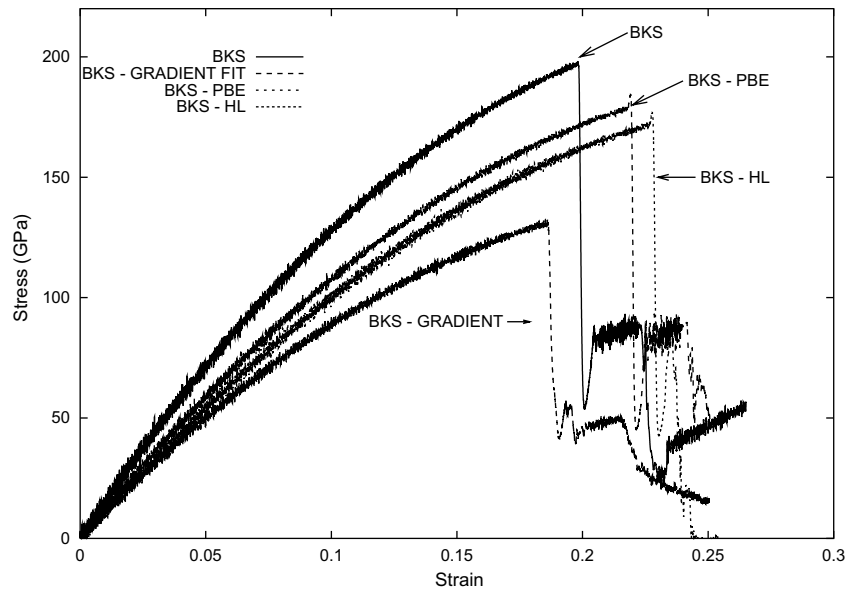


Fig. 4. Computed stress–strain curves for the 216-atom silica nanorod with BKS potential using published BKS parameters and using BKS-type fits to α -quartz DFT results and to CCSD(T) gradients for the “tetrahedrally constrained” H_4SiO_4 .

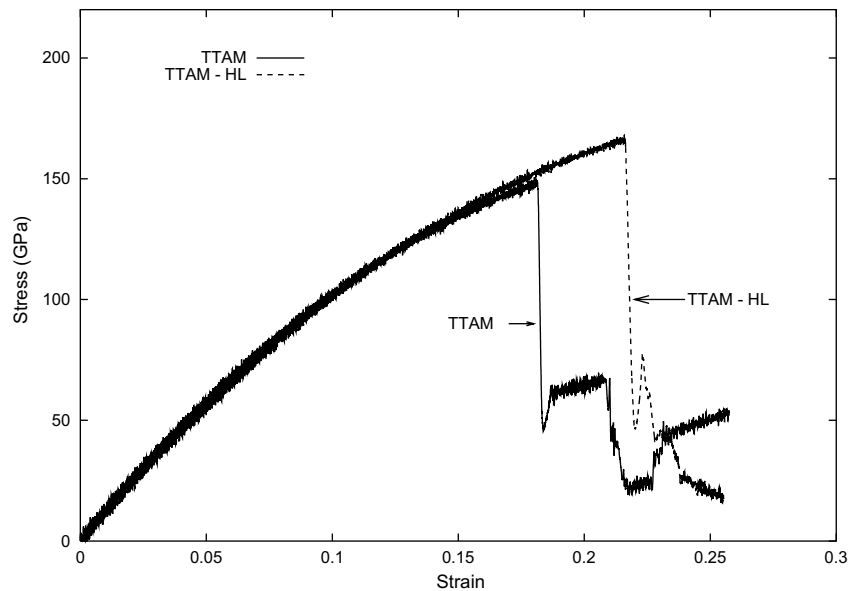


Fig. 5. As in Fig. 4, but for TTAM-type fit to α -quartz as compared to results for the TTAM potential as published.

In general the fitted TTAM systems fail “at once”: beyond the yield strain the stress is essentially independent of strain. In marked contrast, the system with *published* TTAM parameters and *all* the systems with BKS-style parameters generate failure that seems to be related to individual bonds (pair attractions): notice the sawtooth of failure and partial rebound. This is a clear *qualitative* difference generated simply by a change in parametrization. Since the failure mechanisms of nanorods are not the focus of this work, we eschew further analysis.

Previously we had reported [28] that the TTAM-type parametrization for the PBE-DFT (generalized gradient approximation) α -quartz data (“TTAM-PBE”) did not

give a stable nanorod. TTAM-HL does. This instability was for the $T = 5$ K MD, not for $T = 0$ K pure energy minimization. Even after re-examination, however, we have not found any fitted parameter set for TTAM-PBE that will give a stable $T = 0$ K configuration. This difference between TTAM-style fits to data from different DFT XC approximations is a striking sensitivity. Recall from Ref. [14] that the PBE and HL exchange correlation models give calculated α -quartz properties that differ rather modestly. The differences are quantitative, not qualitative. Yet those seemingly modest shifts are enough to have a qualitative impact on the simulation predictions generated by the fitted potentials.

A subtle general characteristic of all these curves is their evident curvature from about ten percent of yield strain all the way to failure. This is considerably more nano-scale ductility than found in full QM calculations on the same system [24]. Again there are implications for embedding. As long as the local strain is in the linear stress–strain region, the embedding should be comparatively straightforward. A problem would arise if the QM were substantially more brittle than the MD; consider for example a fracture simulation.

None of the TTAM-style parameters fit to $\text{H}_6\text{Si}_2\text{O}_7$ via fitting both Si–O and Si–Si together give a stable $T = 0$ K nanorod. Comparison of the parameter values in Table 4 with the published TTAM values shows why. Without a more extensive exploration of the configuration space of $\text{H}_6\text{Si}_2\text{O}_7$, we see no way of getting a useful parametrization from that cluster. The obvious barrier is computational cost.

3.3. Combining cluster and crystalline data

We did not study fits to cluster and bulk data together because of method incompatibility. The problem is related to the systematic, unbounded error growth found when intertwining methods in calculating surface energies [29]. In view of the qualitative differences in MD calculations caused by the relatively modest difference in two DFT models, we see no merit in combining data from DFT and CCSD(T) calculations into one fit. Even if that procedure were to work in this case, there could be no assurance of its generality. It also would be at odds with the objective of embedding a QM region in the best possible classical region. Since only one QM method would be used in a given region, there is little relevance to concurrent fitting to results of several distinct QM calculations in the same region.

4. Conclusions

Most potentials are developed for the purpose of doing MD alone. That not only avoids any need for explicit QM, but actually allows parameter values that might be difficult to extract or even justify from QM calculations on a particular set (usually small) of reference systems. Predictive, first-principles simulations obviously cannot exploit this logical loophole. In particular, multi-scale embedding strategies must aim to have a large CM region that differs as little as possible from the smaller, embedded QM region. Consistency requires that this be true even in those circumstances when the QM region, for some other reason, does not give experimentally valid results.

It would be preferable to have an embedding strategy that did most of its work in stand-alone QM calculations prior to a specific simulation. Put simply, it would be highly desirable to have a generic silica embedding potential pre-calibrated to a selected first-principles QM approximation. The present work shows that there are severe

difficulties with that approach. First, there are reference systems and QM approximations that, in combination with a plausible potential form, fail completely to reproduce the most basic QM outcome, a stable equilibrium structure. A satisfactory embedding strategy must screen out such combinations of systems and potentials. Second, there are large difference in parameter sets that correspond to seemingly modest differences in the choice of method and technical details (basis set size for example). Yet for an a priori scheme to work, it is crucial not to depend upon significant intervention by the user.

In a multi-scale simulation, the benefit of the CM potential is that it avoids explicit consideration of the electronic degrees of freedom. This strategy cannot succeed for *all* properties of the system. The issue then becomes, which properties are to be calculated and to what accuracy? There is also the issue of transferability of the potential. This work shows that re-fitting popular existing forms of SiO_2 potentials to a more limited, though higher quality first-principles database, does not necessarily yield better potentials. It might be that use of a mixed data set, i.e. one having both cluster and bulk data, would be a good strategy. But, as we have just discussed, to avoid incompatible QM approximations, present-day computational costs would restrict any such mixed approach to DFT calculations. Highly refined QM approximations, such as coupled-cluster methodology, simply cost too much to be applied to any but the simplest bulk systems.

If the pre-calibrated embedding potential approach is to succeed at all, it will require at least two other kinds of progress. The harder task is to find a reliable, systematic way of identifying a crucial reference system or systems. The issue is illustrated by the fact that the particular potential used here requires a tetrahedrally constrained H_4SiO_4 . Another illustration is the potential expense of an adequate $\text{H}_6\text{Si}_2\text{O}_7$ calibration data set. More realistic potential functions also will be essential, yet they must be simple enough to allow an embedding to be developed swiftly and not as a significant research project per se. Based on the present work, we are dubious about the prospects for such a multi-scale strategy. What appears to be a more promising multi-scale approach is discussed in Ref. [30].

Acknowledgements

We thank R.J. Bartlett, H.-P. Cheng, P. Deymier, J.W. Dufty, F.E. Harris, M.G. Cory, A. Mallik, J.H. Simmons for helpful discussions. This work was supported by the US National Science Foundation under ITR Award DMR-0325553 and KDI Award DMR-9980015.

References

- [1] J.M. Haile, *Molecular Dynamics Simulation: Elementary Methods*, John Wiley and Sons, New York, 1992 (1997).
- [2] Ways of incorporating quantum mechanics explicitly in MD simulations are well known but far too computationally demanding to be

- generally applicable. Two examples are L. Ye, H.-P. Cheng, *J. Chem. Phys.* 108 (1998) 2015;
R. Car, M. Parrinello, *Phys. Rev. Lett.* 55 (1985) 2471.
- [3] M. Schaible, *Crit. Rev. Sol. State Mater. Sci.* 24 (1999) 265.
- [4] B.P. Feuston, S.H. Garofalini, *J. Chem. Phys.* 89 (1988) 5818.
- [5] L. Huang, J. Kieffer, *J. Chem. Phys.* 118 (2003) 1487.
- [6] S. Tsuneyuki, M. Tsukada, H. Aoki, Y. Matsui, *Phys. Rev. Lett.* 61 (1988) 869.
- [7] B.W.H. van Beest, G.J. Kramer, R.A. van Santen, *Phys. Rev. Lett.* 64 (1990) 1955.
- [8] G.J. Kramer, N.P. Farragher, B.W.H. van Beest, R.A. van Santen, *Phys. Rev. B* 43 (1991) 5068.
- [9] Examples include K. Trachenko, M.T. Dove, *J. Phys.: Cond. Matter* 14 (2002) 7449, and references therein;
M. Benoit, S. Ispas, P. Jund, R. Jullien, *Euro. Phys. J.B* 13 (2000) 631, and references therein;
plus refs in Ref. [5] and those discussed by P. Tangney, S. Scandolo, *J. Chem. Phys.* 117 (2002) 8898.
- [10] T. Watanabe, H. Fujiwara, H. Noguchi, T. Hoshino, I. Ohdomari, *Jpn. J. Appl. Phys.* 38 (1999) L366.
- [11] P. Vashishta, R.K. Kalia, J.P. Rino, I. Ebbsjö, *Phys. Rev. B* 41 (1990) 12197.
- [12] D.W. Brenner, *Phys. Status Solidi B* 217 (2000) 23.
- [13] A.R. Al-Derzi, M.G. Cory, K. Runge, S.B. Trickey, *J. Phys. Chem. A* 108 (2004) 116789.
- [14] N. Flocke, Wuming Zhu, S.B. Trickey, *J. Phys. Chem. B* 109 (2005) 4168.
- [15] R.L. Coldwell, G.J. Bamford, *The Theory and Operation of Spectral Analysis using ROBFIT*, American Institute of Physics, New York, 1991.
- [16] S.A. Alexander, R.L. Coldwell, in: W.A. Lester (Ed.), *Recent Atomic Calculations Using Variational Monte Carlo*, World Scientific Publishing, Singapore, 1997, p. 39.
- [17] W.H. Press, S.A. Teukolsky, W.T. Vetterling, B.P. Flannery, *Numerical Recipes in C++; The Art of Scientific Computing*, second ed., Cambridge University Press, Cambridge, UK, 2002, p. 688.
- [18] M.D. Newton, G.V. Gibbs, *Phys. Chem. Miner.* 6 (1980) 221.
- [19] G.V. Gibbs, *Amer. Mineral.* 67 (1982) 421.
- [20] W. Wong-Ng, G.S. White, S.W. Freiman, *J. Am. Ceram. Soc.* 75 (1992) 3097.
- [21] D.E. Taylor, M.G. Cory, R.J. Bartlett, W. Thiel, *Comput. Mater. Sci.* 27 (2003) 204.
- [22] ACES II is a program product of the Quantum Theory Project, University of Florida. Authors: J.F. Stanton, J. Gauss, S.A. Perera, J.D. Watts, M. Nooijen, Anthony Yau, N. Oliphant, P.G. Szalay, W.J. Lauderdale, S.R. Gwaltney, S. Beck, A. Balková, D.E. Bernholdt, K.-K. Baeck, P. Rozyczko, H. Sekino, C. Huber, Jiříá Pittner, R.J. Bartlett. Integral packages included are VMOL (J. Almlöf, P.R. Taylor); VPROPS (P. Taylor); ABACUS (T. Helgaker, H.J.Aa. Jensen, P. Jørgensen, J. Olsen, P.R. Taylor).
- [23] S.B. Trickey, J.A. Alford, J.C. Boettger, in: J. Leszczynski (Ed.), *Computational Materials Science, Theoretical and Computational Chemistry*, vol. 15, Elsevier, Amsterdam, 2004, p. 171, and references therein.
- [24] Ting Zhu, Ju Li, S. Yip, R.J. Bartlett, S.B. Trickey, N.H. de Leeuw, *Mol. Simul.* 29 (2003) 671.
- [25] C. Zhu, R.H. Byrd, P. Lu, J. Nocedal, Tech. Report NAM-11, EECS Department, Northwestern University, 1994.
- [26] Ju Li, Ting Zhu, unpublished.
- [27] M.P. Allen, D.J. Tildesley, *Computer Simulation of Liquids*, Clarendon Press, Oxford, 1999, p. 74 and Appendix E. We used the corrector coefficients from p. 162, Haile [1].
- [28] S.B. Trickey, A.R. Al-Derzi, N. Flocke, Wuming Zhu, M.G. Cory, K. Runge, Ting Zhu, Ju Li, S. Yip, *Bull. Am. Phys. Soc.* 47 (2002) 1018-S27.
- [29] J.C. Boettger, John R. Smith, U. Birkenheuer, N. Rösch, S.B. Trickey, J.R. Sabin, S. Peter Apell, *J. Phys.: Cond. Matter* 10 (1998) 893.
- [30] A. Mallik, D.E. Taylor, K. Runge, J.W. Dufty, *Int. J. Quantum Chem.* 100 (2004) 1019;
A. Mallik, K. Runge, J.W. Dufty, H.-P. Cheng, *Mol. Simulat.* 31 (2005) 695;
A. Mallik, D.E. Taylor, K. Runge, J.W. Dufty, H.-P. Cheng, *J. Comput. Aided Mater. Des.*, in press.